Theor Chim Acta (1988) 74: 137–150

Theoretica Chimica Acta

MINDO/SR calculations of nickel surface properties as a function of hydrogen coverage

Fernando Ruette[1] and George Blyholder[2]

[1] Centro de Quimica, Instituto Venezolano de Investigaciones Cientificas, I.V.I.C, Apartado 21827, Caracas 1020-A, Venezuela
[2] Department of Chemistry, University of Arkansas, Fayetteville, AR 72701, USA

(Received August 12, 1986, revised September 10, 1987/Accepted November 19, 1987)

The MINDO/SR method is used to study surface properties such as the work function, heat of adsorption and magnetic moment as a function of hydrogen coverage. A good correlation between theory and experiment is found. Furthermore, a qualitative analysis of surface geometry changes due to hydrogen chemisorption is presented.

Key words: MINDO/SR — Nickel — Hydrogen — Surface — Coverage — Work function — Magnetism — Heat of adsorption

1. Introduction

Hydrogen plays an important role in catalytic reactions for many industrial processes of organic molecules where a nickel catalyst is involved. The importance of Ni–H interactions is manifested in a series of experimental and theoretical works [1–11] where a single crystal Ni(100) surface is chosen as a model of hydrogen absorbent.

The present work is a continuation of previous contributions on the chemisorption and diffusion of a single H atom [12], the physisorption, chemisorption and dissociation of an H_2 molecule [13], the interpretation of the UPS difference spectrum [14] and the processes of hydrogen diffusion, charge transfer, phase changes, and thermal desorption [15] on a Ni(100) surface which was modeled by a Ni_{14} cluster. Here, our attention is focused on a qualitative study of some property changes: work function, heat of adsorption and magnetic moments as

the coverage increases. A study of how the surface geometry changes due to hydrogen chemisorption is also presented here.

Our results indicate that in spite of using a cluster with a small number of atoms, there exists a very good qualitative correlation between the above mentioned macroscopic properties and the corresponding calculated microscopic ones.

2. Calculational details

As in previous papers [12–16], the method used is the MINDO/SR-UHF [17]. This method is an adaptation of MINDO/3 [18] to transition metals. The highlight features of the method and methodology are:

(a) The two-center resonance integrals, β_{ij}, are proportional to S_{ij}/R, where S_{ij} and R are the overlap integral and the internuclear distance, respectively.

(b) A linear extrapolation procedure is used in order to obtain α and β parameters that reproduce experimental dissociation energy and equilibrium bond length of transition metal diatomic molecules. A small adjustment of the Slater-Condon parameters is done in order to get a sensible cohesive energy for the nickel cluster.

(c) Different parameters for different atomic orbitals, Ohno-Klopman approximation [19] for two-center repulsion integrals, and a parametric function for the core-core repulsion [18] were used here.

(d) Special attention was taken in the determination of diatomic molecules and clusters ground states by calculating many electronic configurations.

The parameters employed here have been presented in detail elsewhere [20]. All calculations start the SCF process with a density matrix coming from a Ni_{14} cluster calculation [12–13] using the cluster depicted in Fig. 1. The hydrogen chemisorption positions are labelled by the latin letter *A*, *B*, *C*, etc., The subscripts

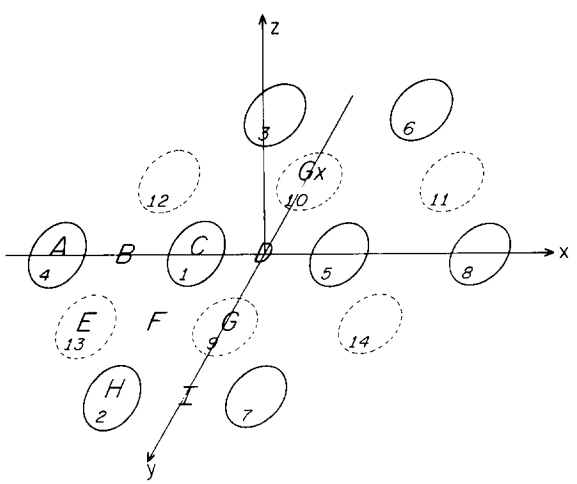

Fig. 1. Ni_{14} nickel cluster and selected adsorption sites

"X" and "Y" indicate symmetric sites obtained by reflection through the XZ and YZ planes as shown in Fig. 1. The optimized Ni-H bond distance (1.70 Å) obtained from previous calculations [12] of a single hydrogen atom on the two-center positions, *B*, *D*, *F*, *I* of the Ni_{14} cluster were used to carry out calculations. This Ni-H distance is considered fixed because in previous work [15] all stable arrangements of two chemisorbed hydrogens, on the same Ni_{14} cluster, have almost the same Ni-H equilibrium bond distances as the case of one single hydrogen [12].

One of the purposes of this work and previous contributions [12-16] is to gather information about the qualities and faults of the MINDO/SR method and our surface model (cluster) for studying chemisorption processes to predict catalytic and surface properties.

3. Changes of surface properties due to coverage

In general, one important aspect in the study of surface science is the effect of the coverage on surface properties. In order to investigate the effects of hydrogen coverage on a nickel surface, several calculations were performed with one to five hydrogens adsorbed over two-fold center sites. Although the adsorption sites that have been selected might not be the most stable ones [12], we choose them because the differences in energy between the two-fold center and the four-fold center (the most stable one) are very small [12]. This is experimentally evident [6] because the hydrogens are able to diffuse on the surface passing through four- and two-fold centers [13]. One important advantage of this choice is the fact that it enables the same cluster from previous work to be used, and this cluster has a sufficient number of two-fold center sites available for adsorption.

Thus, the calculations are started with one adsorbed hydrogen on the most stable site which is a two-fold center site (I) [13]. Then progressively more hydrogens are added to the surface in the most stable remaining sites until saturation on the cluster surface is reached. For each $Ni_{14}H_n$ ($n = 1, \ldots, 5$) system, the most stable multiplicity was obtained. The results of these calculations are presented in Table 1.

Table 1. Properties of the $Ni_{14}H_n$ systems ($n = 0, \ldots, 5$)

Hydrogen adsorption sites	Cluster	Charge on HI	Total charge	E(HOMO) (a.u.)	Heat of adsorp. Kcal/mol	Multi-plicity
—	Ni_{14}	—	—	−0.1074	—	17
I	$Ni_{14}H$	−0.239	−0.239	−0.1250	−57.6	16
I, B	$Ni_{14}H_2$	−0.250	−0.422	−0.1395	−52.6	15
I, Ix, B	$Ni_{14}H_3$	−0.201	−0.582	−0.1536	−43.6	14
I, Ix, B, Bx	$Ni_{14}H_4$	−0.179	−0.668	−0.2182	−47.2	15
I, Ix, B, Bx, D	$Ni_{14}H_5$	−0.118	−0.599	−0.1975	−19.4	14

In what follows, a study of the changes of total energies, total spin, electronic charge transfer, highest occupied molecular orbital (HOMO) energy, diatomic and monatomic energies are related to the corresponding changes in the heat of adsorption, magnetic moment and work function.

3.1. Work function

The simplest way to calculate work function changes induced by adsorbates is by means of a classical model [21–23]. In this model the work function changes due to the adsorption are interpreted as a consequence of the resulting dipole layer from the charge transfer between substrate and adatoms. The work function change ΔWF is related to the surface adatom density D through the Helmholtz's equation

$$\Delta \mathrm{WF} = 4\pi D d, \tag{1}$$

where d is the dipole moment perpendicular to the surface. For covalent adsorption with partial ionic character, the variable d is obtained as δr, where δ is the fractional charge transferred by the adsorbate atom and r is the perpendicular charge separation between the adsorbate and the metallic surface. From the above expression, it is clear that ΔWF is directly proportional to the total amount of charge transferred.

In the third and fourth columns of Table 1, the electronic charge density of a single hydrogen atom adsorbed on the site I and the total charge of all hydrogens adsorbed on each one of the $Ni_{14}H_n$ systems are presented. It is observed that the total electronic charge density carried by the hydrogens is incremented as the coverage becomes greater while the charge over a single hydrogen decreases when other hydrogens are adsorbed near by.

Because the Ni–H bond distances are considered to be constant, see sect. 2, a plot of the total hydrogen electronic charges vs. the number of adsorbed hydrogens will give information on how the work function changes as the coverage varies (see Fig. 2). It is evident from Fig. 2 that at small coverages, the variation of the work function is nearly linear. A similar behavior has been reported experimentally by Christmann et al. [24]. If the adsorption patterns shown at the bottom of Fig. 2, are repeated all over the surface, we might associate the coverage of $\theta = 0.5$ to the cluster with four hydrogens. Thus, from Fig. 2, we observe that at coverages close to and smaller than $\theta = 0.5$ ΔWF starts to behave not linearly, and for coverages greater than 0.5 the ΔWF values diminish. These theoretical trends also match very closely the experimental ones [21, 24].

The work function (WF) is defined as the difference in energy of one electron in the bulk metal at the Fermi level and at the vacuum level outside the surface [25]. Based on this definition, another simple way to evaluate the WF changes is to use HOMO energy. For this reason, the HOMO energy values are listed in column five of Table 1 and are plotted vs. the number of adsorbed hydrogens in Fig. 2. The results indicate that the WF has a linear behavior at small coverage which is in agreement with the above results. As the coverages increases, the WF becomes larger until it reaches a point, close to saturation, where it starts to decrease.

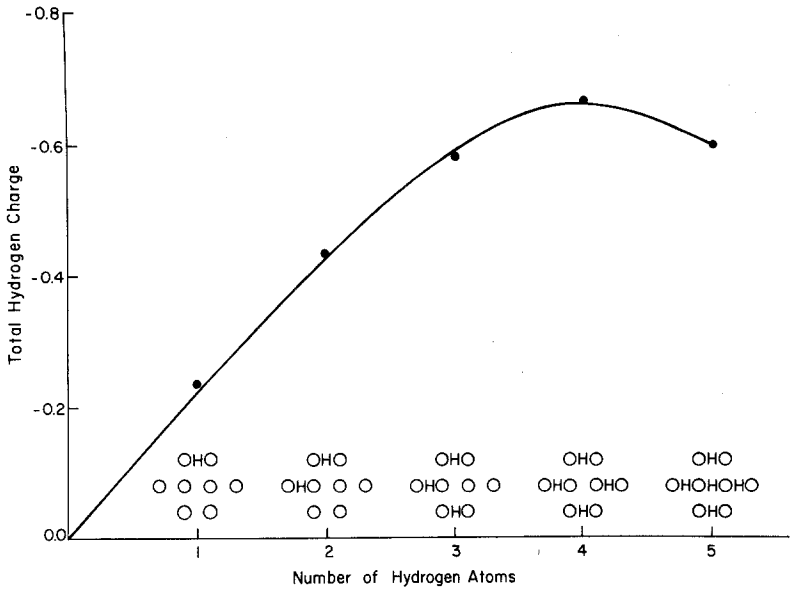

Fig. 2. Total hydrogen charge against the number of adsorbed hydrogens

An explanation of this WF increases with the coverage may be given by the effects of the electronic charge transfer from the adsorbent (cluster) to the adsorbates (hydrogens). This transfer creates an electrostatic potential that is opposed to the extraction of an electron from the cluster. The electron withdrawal from the nickel cluster is essentially from the sp-orbitals since the *d*-orbital population remains almost constant [15]. In addition, the HOMOs are formed by H(*s*) and Ni(*sp*) orbitals spread out through the cluster, therefore, they are directly affected by the electronic *sp*-withdrawing. Thus, there is a good correlation between charge transfer at small coverage and HOMO stability, because, a larger charge transfer corresponds to a larger HOMO energy. Another feature which is important to account for is the WF change close to saturation ($\theta \approx 1$). In a previous paper [15], it was proposed that the interaction of two adsorbed hydrogens on a Ni_{14} cluster is due to charge separation in the zones close to adsorption sites. In other words, the adsorption of a hydrogen atom produces a region of influence around its adsorption site, so, if a second hydrogen atom is adsorbed near by, they should interact through the cluster according to the separation distance between them. Thus, the adsorption of another hydrogen atom on the $Ni_{14}H_4$ cluster to reach saturation ($Ni_{14}H_5$) conduces to a greater H-H indirect interaction because of the following facts:

(a) There are smaller H-H distances in $Ni_{14}H_5$ (2.50 Å) than in $Ni_{14}H_4$ (3.53 Å).

(b) More than one hydrogen atom is directly attached to a nickel atom (hydrogens on sites *B* and *D* are bound to the nickel atom number 1, and those on sites *D* and B_y are bonded to the atom 5).

These facts lead to a decrease of the total charge transfer, as shown in Fig. 2, which causes also a dwindling of the HOMO energy as indicated in Fig. 3.

In conclusion, the two models (total charge transfer and HOMO energy), used here to study WF changes have a similar behavior with the coverage, except an unexpected increase of the $Ni_{14}H_4$ HOMO energy which is explained in the following section by studying mono- and diatomic energies.

3.2. Heat of adsorption

The hydrogen adsorption over a Ni_{14} cluster may be represented by the reaction

$$Ni_{14} + n/2H_2 \rightarrow Ni_{14}H_n.$$

In general, the heat of adsorption, ΔBE, is related to the energy of the molecules involved in the chemisorption by the following equation:

$$\Delta BE = 2/n(E(Ni_{14}H_n) - E(Ni_{14})) - E(H_2), \tag{2}$$

where n is the number of adsorbed hydrogens. $E(Ni_{14}H_n)$, $E(Ni_{14})$, and $E(H_2)$ are the total energies of the $Ni_{14}H_n$, Ni_{14}, and H_2 systems respectively.

In column six of Table 1, the ΔBE values are presented and are then plotted against the number of adsorbed hydrogens as shown in Fig. 4. It is observed that at small coverages ΔBE moderately decreases as the number of adsorbed hydrogens increases until a coverage value greater and close to 0.5 is reached, where ΔBE rapidly diminishes. Experimental results [24] also indicate that at very small coverage the heat of adsorption diminishes but with increasing coverage ΔBE is maintained almost constant until it reaches a point where it suddenly decreases. This abrupt ΔBE change has been interpreted by Christmann et al. [24] and in previous papers [15-16] as the filling of the β_1 state that appears in the TPD spectra and corresponds to a coverage of $\theta = 0.5$ [21]. In general, the behaviour of the heat of adsorption with coverage is similar to that obtained experimentally.

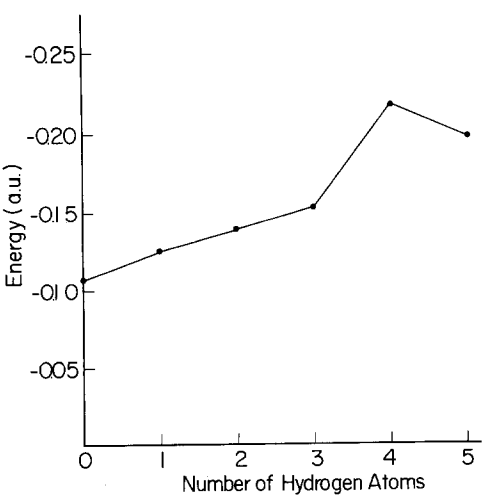

Fig. 3. HOMO energy against the number of adsorbed hydrogens

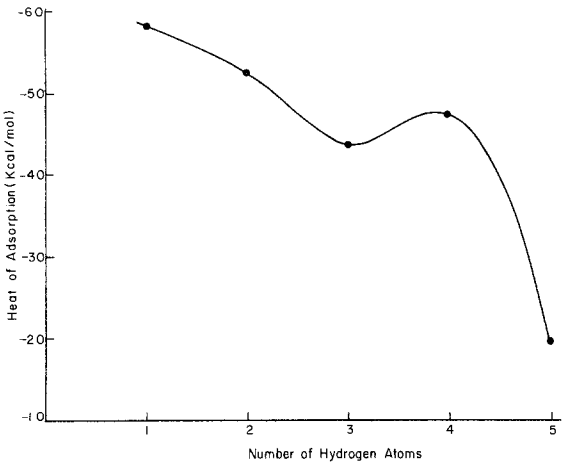

Fig. 4. Heat of adsorption as a function of the number of adsorbed hydrogens

Nevertheless, in our cluster the observed changes due to the hydrogen adsorption are more pronounced.

An analysis of ΔBE changes caused by the hydrogen coverage is carried out by considering the energetic interactions between the atomic species that form the adsorbate and adsorbent. The total diatomic energies between Ni atoms (E(Ni-Ni)), H atoms (E(H-H)), and Ni and H atoms (E(Ni-H)) are presented in Table 2. In addition, the total monoatomic energies for the Ni (E(Ni)) and H (E(H)) atoms are also included. The E(Ni-Ni) and E(Ni) values are calculated with respect to the corresponding ones of the clean cluster (Ni_{14}). In a similar way, the E(H) values are evaluated with respect to the corresponding free hydrogen atom energies. At this point, it is good to have in mind, according to Eq. 2, the necessary energy to dissociate a hydrogen molecule. In order to analyze in an easy way these results, in Fig. 5, a plot of the total diatomic and monoatomic energies vs. the number of adsorbed hydrogens is presented. The positive values of E(Ni-Ni), E(Ni) and E(H) indicate an energetic instability with respect to the clean cluster and free hydrogens, respectively. On the other hand, negative values of E(Ni-H) show that there is a strong stabilization owing to the Ni-H interaction. It is good to note that the E(H-H) term makes a small contribution to the ΔBE decrease, hence, it indicates that the coverage influence in BE values is not a consequence of the direct H-H interaction but a series of effects that are

Table 2. Diatomic and monoatomic energies (a.u.)

Cluster	E(H-H)	E(Ni-H)	E(Ni-Ni)	E(Ni)	E(H)
$Ni_{14}H$	—	−0.37633	+0.14387	+0.03242	+0.07130
$Ni_{14}H_2$	+0.00726	−0.75937	+0.26466	+0.09286	+0.14743
$Ni_{14}H_3$	+0.01296	−1.13768	+0.43863	+0.09751	+0.24198
$Ni_{14}H_4$	+0.02045	−1.54946	+0.58377	+0.13249	+0.33643
$Ni_{14}H_5$	+0.01666	−1.83917	+0.67817	+0.19824	+0.46007

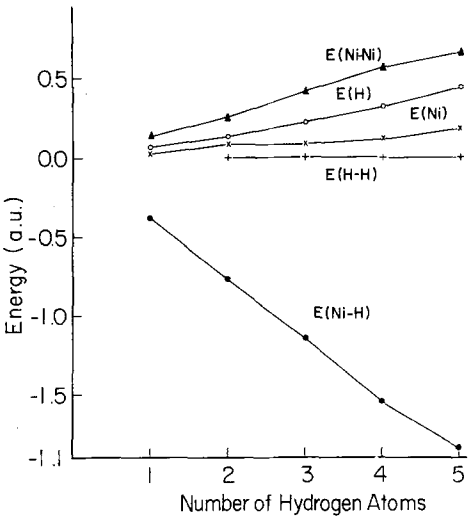

Fig. 5. Diatomic and monoatomic energy terms with the coverage

transmitted through the cluster, see variation of E(Ni-Ni), E(Ni) and E(H) shown in Fig. 5. Similar results have been reported for the adsorption of two hydrogen atoms on the same nickel cluster [15].

The E(Ni-Ni) increase with the coverage, see Fig. 5, may be account for the fact that according to these results, previous [12], and experimental ones [26], the Ni-Ni bonds are constituted of *sp*-orbitals and the electronic charge transfer is in fact coming from the nickel *sp*-orbitals. This charge transfer gives rise to a decrease of the Ni-Ni bonding population which produces a weakening of the Ni-Ni bonds respect to the nickel clean cluster.

In order to visualize in more detail the ΔBE behavior in the region close to saturation, a plot of variation of the diatomic and monoatomic energy changes vs. the number of hydrogen atoms adsorbed is presented in Fig. 6. Let us analyze what occurs when the fourth hydrogen is adsorbed: ΔE(Ni-Ni) and ΔE(Ni)

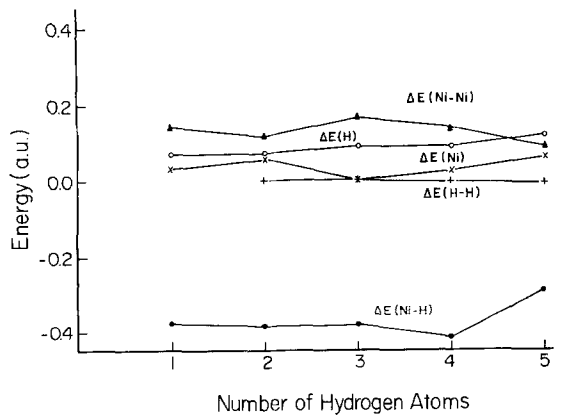

Fig. 6. Diatomic and monoatomic energy changes with the coverage

terms cancel each other, $\Delta E(\mathrm{H})$ remains constant, and, therefore, $E(\mathrm{Ni\text{-}H})$ is responsible for the ΔBE increase shown in Fig. 4. A similar increase in the HOMO energy is also observed, as shown in Fig. 3. If the fifth hydrogen is adsorbed, the dominant term $E(\mathrm{Ni\text{-}H})$ decreases, yielding the ΔBE diminishing shown in Fig. 4 and consequently the decrease of HOMO energy depicted in Fig. 3. Therefore, there is a correlation between the $E(\mathrm{Ni\text{-}H})$ and the HOMO energy which may be explained by the fact that as HOMOs as Ni-H bonds in all clusters are made up of Ni(sp) and H(s) orbitals.

3.3. Magnetic moment

It is well-known that the magnetic properties of transition metals are related to the number of spin up and spin down electrons. For this reason in these calculations we take special care to obtain the most stable multiplicities for each one of the clusters, see the last column in Table 1. The multiplicity value for the Ni_{14} cluster is 17 which gives a spin magnetic moment of about 1.1. μ_B. This value is high compared to experimental results for the bulk (0.56 μ_B) [27]. Two main causes may be responsible for this high value of magnetic moment: (i) the tendency of HF calculations to be biased in favor of states with high multiplicity [28], for example, *ab-initio* calculations [29] for a Ni_6 cluster produce a magnetic moment of 1.3 μ_B; (ii) there is experimental evidence of an enhancement in the magnetic moment for surface nickel atoms [30-31]. Recent calculations using a modified SCF-Xα-SW [32-33] and slab-type methods [34-35] lead to values of magnetic moment close to the experimental value. On the other hand, slab-type calculations [36] reveal that the magnetic moment for Ni(100) and Ni(110) monolayers results to be 0.86 μ_B and 0.96 μ_B respectively, and density functional theory calculations [37] report values of 1.14 and 0.80 μ_B for Ni_{13} and Ni_{19} clusters, respectively.

It is experimentally known that nickel magnetization decreases after hydrogen chemisorption [25] which indicates a pairing of the surface electrons with the electron of the adsorbed hydrogen. In order to easily analyze the effect of hydrogen chemisorption, in Fig. 7, a plot of the fraction of the added electrons from

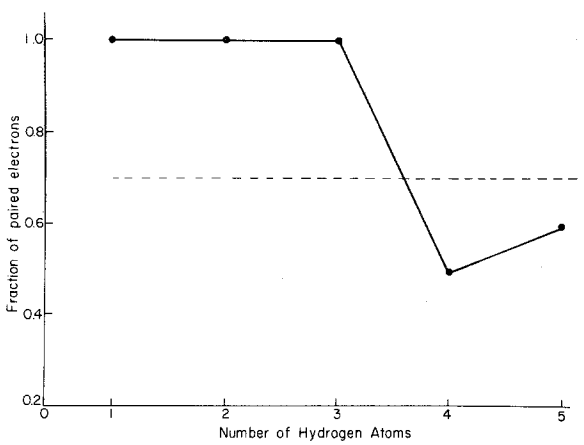

Fig. 7. Fraction of paired electrons vs, the number of adsorbed hydrogens

hydrogen which are paired vs. the number of adsorbed hydrogens, is presented. Although, the number of hydrogens is small, it is observed that the resultant saturation fraction of paired electrons (0.6) is close to the experimentally reported value (0.7) [25].

With the purpose to understand in more detail the hydrogen chemisorption effects on the magnetism, in Table 3, the *sp*- and *d*-spin densities for each atom of the $Ni_{14}H_n$ ($n=0,\ldots,5$) clusters are presented. The more important features and conclusions are enumerated as follows:

(a) The spin density on *d* orbitals is maintained nearly constant after the hydrogen adsorption. Each atom has a *d*-spin density of about 1 which is consistent with a $d^9(sp)^1$ configuration of the nickel atoms [13].

Table 3. Atomic spin densities for $Ni_{14}H_n$ ($n=0,\ldots,5$). For each nickel atom, the following two rows correspond to *d*- and *sp*-spin densities respectively. Atoms 15–19 are hydrogens

Atom	Ni_{14}	$Ni_{14}H$	$Ni_{14}H_2$	$Ni_{14}H_3$	$Ni_{14}H_4$	$Ni_{14}H_5$
1	−0.999	−0.991	−0.991	−0.992	−0.994	−0.993
	−0.103	−0.114	−0.010	−0.022	−0.004	−0.023
2	−0.992	−0.983	−0.982	−0.975	−0.980	−0.980
	−0.143	−0.022	−0.016	0.047	−0.017	−0.007
3	−0.992	−0.989	−0.989	−0.981	−0.908	−0.980
	−0.143	−0.016	−0.011	0.128	−0.017	−0.007
4	−0.997	−0.997	−0.989	−0.989	−0.990	−0.990
	−0.318	−0.315	0.003	0.025	−0.012	0.107
5	−0.999	−0.991	−0.990	−0.992	−0.994	−0.993
	−0.103	−0.114	−0.014	−0.022	−0.004	−0.023
6	−0.992	−0.989	−0.989	−0.981	−0.980	−0.980
	−0.143	−0.016	0.003	0.128	−0.017	−0.007
7	−0.992	−0.983	−0.982	−0.975	−0.980	−0.980
	−0.143	−0.022	−0.005	0.047	−0.017	−0.007
8	−0.997	−0.997	−0.994	−0.989	−0.990	−0.990
	−0.318	−0.316	−0.057	0.025	−0.012	−0.107
9	−0.993	−0.994	−0.994	−0.992	−0.994	−0.994
	−0.131	−0.056	−0.001	0.095	−0.007	0.033
10	−0.993	−0.995	−0.994	−0.985	−0.994	−0.994
	−0.131	−0.052	0.002	0.158	−0.007	0.033
11	−0.990	−0.989	−0.990	−0.993	−0.994	−0.993
	−0.104	−0.074	−0.023	0.000	−0.009	0.039
12	−0.990	−0.989	−0.993	−0.993	−0.993	−0.993
	−0.104	−0.074	−0.006	0.000	−0.009	0.039
13	−0.990	−0.987	−0.992	−0.991	−0.993	−0.993
	−0.104	−0.073	−0.003	0.026	−0.009	0.039
14	−0.990	−0.987	−0.988	−0.991	−0.993	−0.993
	−0.104	−0.073	−0.017	0.026	−0.009	0.039
15	—	0.001	0.002	0.026	−0.003	−0.003
16	—	—	0.011	0.066	0.006	0.121
17	—	—	—	0.066	0.006	0.121
18	—	—	—	—	−0.003	−0.033
19	—	—	—	—	—	0.199

(b) The magnetic change caused by the hydrogen adsorption is a consequence of variation in the *sp*-spin density.

(c) The *sp*-spin is spread out through the cluster with a tendency of being concentrated on the edge atoms.

(d) The hydrogen adsorption changes the spin density not only on the nickel atoms where hydrogens are directly adsorbed but all over the cluster.

(e) The hydrogen atoms have a small contribution to the total spin density.

(f) The *d*-spin densities on the nickel atoms has the same sign. This suggests that spin correlation of electrons with different spin is not explicitly taken into account in our MINDO/SR-UHF calculations. In fact, this is a fault of all Hartree-Fock type approaches where the Coulomb hole correlation is not included, and only the exchange correlation is considered.

Recently other calculations for magnetic moment changes due to hydrogen chemisorption in nickel surfaces have been performed [32, 38]. In these calculations a considerable reduction of the magnetic moment is reported, which is not observed in our calculations. However, the comparison of different metallic cluster calculations has to take into account the fact that cluster properties, including magnetic ones, change with the size and geometry of the cluster [32, 37, 39-42].

4. Geometrical modifications

From a practical point of view, calculations of nickel clusters with optimization of Ni-Ni distances are not considered here. Nevertheless an analysis of the bond orders and diatomic energy changes may be used to predict trends for the internuclear distances. Here we use an arrangement of two hydrogen atoms (G-G_x) [15] which may be associated with the maximum coverage of 1 [4].

In Table 4, the Ni-Ni bond order changes (BO) and the diatomic energy changes

Table 4. Changes of bond orders (BO) and diatomic energies (DE) for a Ni_{14} cluster upon the adsorption of H_2 on G-G_x centers

Nickel atoms	BO	DE (a.u.)
1- 2	−0.062	−0.0250
1- 4	−0.029	−0.0040
1- 5	−0.045	−0.0223
1- 9	−0.065	−0.0148
1-12	−0.042	−0.0057
2- 7	+0.034	+0.0016
2- 9	+0.006	+0.0030
2-13	+0.064	+0.0148
4-12	−0.005	−0.0001
9-10	−0.038	−0.0065
9-13	−0.033	−0.0041
11-14	−0.062	−0.0203

(DE) between the nearest neighbor nickel atoms in the $Ni_{14}H_2(G-G_x)$ cluster with respect to the corresponding ones in the Ni_{14} cluster are presented. Here, only the necessary pairs of nickel atoms are depicted because the others may be obtained by symmetry. As expected, a very good correlation between the bond order changes and the corresponding diatomic energy changes exists. The results indicate that bond order changes for all atoms bonded to nickel atoms attached to two hydrogens (1 and 5) are negative. This means that the bond distances between atoms 1 and 5 and their nearest-neighbors have a tendency to be longer. On the surface, only the 2–7 bond distance type would be shorter. Bonds between the edge surface atoms and the underlayer atoms tend to be tighter except those that do not have hydrogens chemisorbed on them. The effect of the adsorption goes beyond the toplayer since all bonds between atoms in the underlayer have a tendency to be longer.

A rough picture of how the surface changes as the chemisorption occurs is shown in Fig. 8. Here the dashed circles correspond to the shifted nickel atoms after hydrogen chemisorption and the arrows indicate the direction of the shifting. It is easy to see that all surface nickel atoms have a tendency to move away from the site where hydrogen is chemisorbed, see top view Fig. 8a. In the side view, Fig. 8b it is shown how the nickel atoms bonded to the two hydrogens move above up the XY plane and the edge atoms (2, 3, 6 and 7) are displaced below this plane.

The displacement of the nickel surface atoms may be cuased by the charge transfer to the hydrogens. As we explained in Sect. 3.2, the electronic charge transfer involves Ni(sp) electrons apart from the Ni–Ni bonds are sp-type. Therefore, this redistribution of charge produces a weakening of the Ni–Ni bonds in the region close to the hydrogen adsorption giving rise to a displacement of the nickel atoms above the surface.

As can be seen, this qualitative analysis reveals a reconstruction of the surface atoms of the cluster. Demuth [43] and Christmann et al. [44] report that the adsorption of hydrogen does produce a reconstruction of a Ni surface. These

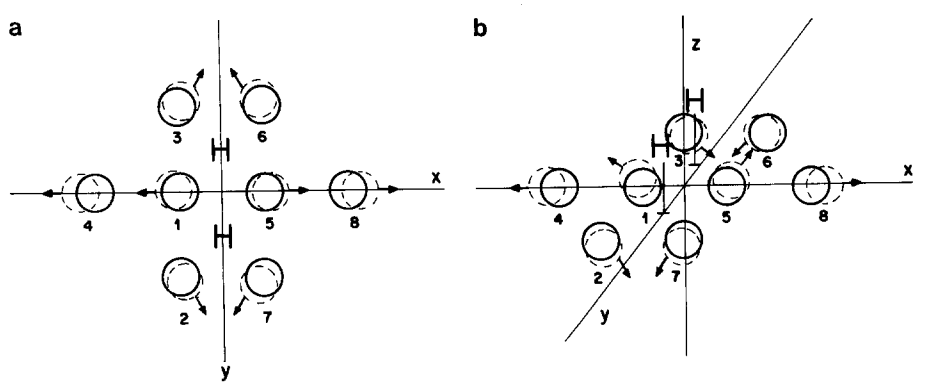

Fig. 8. Displacements of cluster nickel atoms upon hydrogen chemisorption: **a** top view; **b** side view

theoretical trends about the weakening of the nickel surface bonds also correlate well with recent experimental field ion microscope (FIM) results by Wada et al. [45]. They observed that the adsorption of hydrogen in polycrystalline nickel causes a reduction of the evaporation voltage which is attributed to a decrease of the surface binding energy. It should be noted that the tendency of the nickel atoms to be separated may be of great importance for the process of diffusion into the bulk [46-47].

Conclusion

It has been shown that a very simple model of the surface with a limited number of sites and a quite rapid calculational method (MINDO/SR) may be successfully used to qualitatively study the variation of surface properties with coverage. It is known that the property values of a cluster may be different from those of an infinite well-defined surface, for example, catalytic reactivity [39-41, 48, 49], ionization potential [42], electrochemical potential [50] and band structure [51]. However, a cluster with a reasonable number of atoms conserves some property trends which are analogous to actual surfaces.

Acknowledgement. This research could not have been accomplished without CONICIT's donation of a VAX 11-780 computer to IVIC and the computational facilities provided by IBM of Venezuela.

References

1. Knor Z (1982) In: Anderson JR, Boudart M (eds) Catalysis science and technology. Springer, Berlin Heidelberg New York
2. Goodman DW, Kiskinova M (1981) Surf Sci 105:L265; Kiskinova M, Goodman DW (1981) Surf Sci 109:L555; Goodman DW, Kelley RD, Madey TE, Yates JT (1980) J Catal 63:226
3. Koel BE, Peebles DE, White JM (1983) Surf Sci 125:739; Peebles DE, Peebles HC, Belton DN, White JM (1983) Surf Sci 125:709
4. Rieder KH, Wilsch H (1983) Surf Sci 131:245
5. Hellsing B, Mällo A (1984) Surf Sci 144:336
6. Stensgaard I, Jakobsen F (1985) Phys Rev Lett 54:711; George SM, DeSantolo AM, Hall RB (1985) Surf Sci 159:L245
7. Nordlander P, Holloway S, Norskov JK (1984) Surf Sci 136:59
8. Saillard JY, Hoffman R (1984) J Am Chem Soc 106:2006
9. Upton TH (1984) J Am Chem Soc 106:1561
10. Keller J, Castro M, De Paoli AL (1982) J Appl Phys 53:8850
11. Companion AL, Liu F, Onwood DP (1985) J Less-Common Met 107:131; Vargas P, Kronmüller H, Bohm MC (1986) J Phys F 16:L281
12. Ruette F, Blyholder G, Head J (1984) Surf Sci 137:491
13. Ruette F, Hernández A, Ludeña E (1985) Surf Sci 151:103
14. Ruette F, Hernández A, Ludeña EV (1986) Surf Sci 167:393
15. Ruette F, Hernández A, Ludeña EV (1986) Int J Quantum Chem 29:1351
16. Ruette F, Hernández AJ, Sánchez M (1987) In: Castro GR, Cardona M (eds) Lectures in Surface Science. Springer, Berlin Heidelberg New York, pp 120-123
17. Blyholder G, Head J, Ruette F (1982) Theor Chim Acta 60:429
18. Bingham RC, Dewar, MJS, Lo DHJ (1975) J Am Chem Soc 97:1285
19. Ohno K (1964) Theor Chim Acta 2:219 Klopman G (1965), J Am Chem Soc 87:3300

20. Ruette F, Blyholder G, Head J (1984) J Chem Phys 80:2042
21. Christmann K (1979) Z Naturforsch 34a:22
22. Gundry PM, Tompkins FC (1968) Surface potentials. In: Anderson RB (Ed) Experimental methods in catalysis research, vol 1. Academic Press, pp 100–168
23. Hölz J, Schulte FK (1979) Work function of metals. In: Höhler (ed) Tracts in modern physics, vol 85. Springer, Berlin Heidelberg New York, pp 1–140
24. Christmann K, Schober O, Ertl G, Neumann M (1974) J Chem Phys 60:4528
25. Tompkins FC (1978) Chemisorption of gases on metals. Academic Press, London New York San Francisco
26. Morse MD, Hansen GP, Langridge-Smith PRR, Zheng LS, Geusic ME, Michalopoulos DL, Smalley RE (1984) J Chem Phys 80:5400
27. Darmon H, Heer R, Meyer JP (1968) J Appl Phys 39:669
28. Demuynck J, Rohmer MM, Strich A, Veillard A (1981) J Chem Phys 75:3443
29. Bash H, Newton MD, Moskowitz JW (1980) J Chem Phys 73:4492
30. Montano PA, Purdum H, Shenoy GK, Morrison TI, Schulze W (1985) Surf Sci 56:228
31. Stadnik ZM, Griesbach P, Dehe G, Gütlich P, Kohara T, Stroink G (1987) Phys Rev B 35:6588
32. Fournier R, Salahub DR (1986) Int J Quantum Chem 24:1077
33. Salahub DR, Raatz F (1984) Int J Quantum Chem 18:173; Raatz F, Salahub DR (1984) Surf Sci 146:L609
34. Freeman AJ (1983) J Mag Mater 35:31 (and references therein)
35. Wimmer E, Freeman AJ, Krakauer H (1984) Phys Rev 30:3113
36. Krakauer H, Freeman AJ, Wimmer E (1983) Phys Rev B 28:610
37. Lee K, Callaway J, Kwong K, Tang R, Ziegler A (1985) Phys Rev B 31:1796
38. Weinert M, Davenport JW (1985) Phys Rev Lett 54:1547
39. Morse MD, Geusic ME, Heath JR, Smalley RE (1985) J Chem Phys 83:2293; Geusic ME, Morse MD, Smalley RE (1985) J Chem Phys 82:590
40. Richtsmeier SC, Parks EK, Liu L, Pobo LG, Riley SJ (1985) J Chem Phys 82:3659
41. Rohlfing EA, Cox DM, Kaldor A, Johnson KH (1984) J Chem Phys 81:3846
42. Whetten RL, Cox DM, Trevor DJ, Kaldor A (1985) J Phys Chem 89:566
43. Demuth JE (1977) J Colloid Interface Sci 58:184
44. Christmann K, Chelab F, Penka V, Ertl G (1985) Surf Sci 152/153:356
45. Wada M, Uemori R, Nishikawa O (1983) Surf Sci 134:17
46. Latanision RM, Kurkela M (1983) Corrosion 39:174
47. Cox BN, Bauschlicher CW (1981) Surf Sci 180:483
48. Gallezot P (1981) Surf Sci 106:459
49. Van Broekhoven EH, Ponec V (1985) Surf Sci 162:731
50. Plieth WJ (1982) J Phys Chem 86:3166
51. Baetzold RC, Mason MG, Hamilton JF (1980) J Chem Phys 72:366